Fracture 1977, Volume 2, ICF4, Waterloo, Canada, June 19 - 24, 1977

EFFECT OF TEMPERING TREATMENTS ON THE FRACTURE BEHAVIOUR OF A Cr-Mo-V PRESSURE VESSEL STEEL

K. Törrönen and H. Kotilainen*

INTRODUCTION

During the tempering of quenched Cr-Mo-V steels several overlapping microstructural reactions occur. These include recovery of the dislocation structure as well as precipitation, growth and dissolution of various carbides. These microstructural processes introduce drastic changes in the yield and fracture behaviour of the material [1].

Generally several microstructural factors influence the mechanical properties of quenched and tempered steels, the main contributions coming from the grain size and fine carbide dispersion. The relationship between yield strength σ_y and grain size d obeys the Hall-Petch equation [2].

$$\sigma_y = \sigma_i + k_y d^{-1/2} \tag{1}$$

where σ_i is the friction stress. Similar expression exists between fracture stress and grain size [2]. Thus grain refinement increases both the yield and fracture stresses. As the increment of fracture stress is larger, the ductile-brittle transition temperature consequently decreases [3], i.e. both strength and toughness improves.

Fine carbide dispersions produce an increment in the yield stess which is related to the carbide size D and planar spacing L_A between carbides through the Orowan equation. Several improved modifications of this equation have been presented, e.g. the equation by Foreman et al. [4] and Kelly [5].

$$\Delta\tau = \frac{0.83\ G_s b}{2\pi(1-\nu)^{1/2}} (L_A - D)^{-1} \ln \frac{D}{b} \tag{2}$$

and the equation by Bacon et al. [6].

$$\Delta\tau = \left[\frac{\ln \frac{D}{b}}{\ln \frac{L_A - D}{b}}\right]^{1/2} \frac{G_s b}{2\pi(1-\nu)} (L_A - D)^{-1} \ln \frac{D}{b} \tag{3}$$

where G_s is shear modulus. The effect of a fine carbide distribution on fracture stress and toughness, however, still remains rather unclear. There is some evidence that the cleavage fracture stress is increased by fine carbides [7], although a degragation of toughness is also noticed [8].

*Technical Research Centre of Finland, Reactor Materials Research, SF-02150 ESPOO 15, Finland

The superposition of the strengthening due to grain boundaries and carbide distribution has not been fully clarified either. Some previous investigations [7,9] indicate that grain boundary hardening is ineffective if a large number of incoherent and small particles is present.

The present work attempts to elucidate the yield and fracture behaviour observed in a Cr-Mo-V pressure vessel steel after different tempering treatments by correlating the mechanical properties to the microstructural parameters. The applicability of the equations 1 to 3 is also studied.

EXPERIMENTAL PROCEDURE

The amounts of the principal alloying elements in the steel studied were 2.8%Cr, 0.6%Mo, 0.3%V and 0.18%C. Two austenitizing treatments (950°C and 1050°C) and several quenching simulations were performed. Tempering was carried out at the temperature range from peak secondary hardening to near A_{c1}, i.e. at temperatures in the range 600...760°C. Holding times were varied up to 90 h.

Mechanical properties were measured after tempering using room temperature tensile tests, Charpy V impact tests and Pellini drop-weight tests. The critical resolved shear stress was calculated from the 0.2% offset yield stress by dividing with the Taylor factor 2.75 [10].

The microstructural observations were made from thin foils and replicas using transmission electron microscopy at 100 and 200 kV and from optical micrographs. Fracture surfaces were studied by scanning electron microscopy. Several microstructural parameters were measured including the prior austenite grain size, the ferrite grain size, the lath packet width and the lath width (or cell size). The mean size of the carbides as well as the interparticle spacings were also estimated.

RESULTS

Microstructure

The as-quenched microstructure consisted of granular bainite regardless of the quench rate; neither conventional upper or lower bainite nor proeutectoid ferrite could be found. As a result of the two austenitizing temperatures, two prior austenite grain sizes (ASTM 3 and ASTM 6) and correspondingly two ferrite grain sizes (46 µm and 35 µm, respectively) were obtained. However, the lath width (0.43 µm) and the width of lath packet surrounded by high-angle boundaries remained the same (0.9-1.9 µm, mean value 1.33 µm) regardless of the austenitizing treatments [11].

Two size groups of carbides were found. The size of the larger M_7C_3-type carbides never exceeded more than 0.3 µm and they were evenly distributed. No excess precipitation on grain boundaries was found. The fine carbide dispersion was composed of squared plate shaped vanadium-rich MC-carbides. The size of MC-carbides was measured as the mean caliper diameter, i.e. the length of the plate edge.

The cleavage fracture unit size was measured from broken halves of Charpy specimens. The unit size was always the same (mean value 2.3 µm) regardless of different austenitizing, quenching and tempering treatments.

Typical features appearing in a microstructure and cleavage fracture surface are shown in Figure 1, corresponding to a tempering treatment to a Hollomon-Jaffe tempering parameter value about 20500. The effect of tempering on several microstructural parameters is given in Figure 2. The lath packet and grain sizes remained the same throughout the tempering range investigated.

Mechanical properties

Increasing the tempering parameter introduced a drastic drop in yield and tensile strength. Consequently the ductile-brittle transition temperatures (DBTT) as well as the NDT-temperature (NDTT) also decreased as shown in Figure 2. A corresponding increase in Charpy V upper shelf energy and ductility was found. No effect of differing grain sizes on the measured mechanical properties was ever detected, except for the upper shelf energy, which was slightly lowered after higher austenitizing treatments.

DISCUSSION

The planar interparticle spacing of the MC-carbides throughout the investigated tempering range remains the finest microstructural unit (Figure 2). The spacing of the M_7C_3 (and $M_{23}C_6$)-carbides is almost an order of magnitude coarser, and as they remain comparatively small - although larger than MC-carbides - and evenly distributed, it can be assumed that their effect on mechanical properties is negligible. According to the results it can be further supposed that the contribution of grain boundaries to the yield strength is constant or negligible throughout the tempering range studied. Hence it is evident that changes in the spacing of the MC-carbides, which also control the dislocation density, alone determines the changes in yield strength. This is clearly illustrated in Figure 3, where the observed critical resolved shear stress values are plotted as a function of the inverse of a parameter λ, which is defined as

$$\lambda^{-1} = (L_A - D)^{-1} \ln \frac{D}{b} \qquad (4)$$

i.e. this parameter is the planar interparticle surface-to-surface distance corrected with a factor due to dislocation dipole formation [12]. The best fit curve in Figure 3 shows a linear relationship indicating the Orowan relationship. The measured values are in a close agreement with theoretical ones, lying between the linear curve drawn according to equation (2) and values calculated from equation (3).

When the measured Charpy V DBTT and Pellini NDTT-values are plotted as a function of λ^{-1}, a linear relationship is again found (Figure 4). However, at the smallest value of the spacing, when mean carbide size is close to 5 nm, a behaviour diverging from the linearity is observed. This can be explained as a change in deformation mechanism, dislocations starting to penetrate through the carbides instead of bowing around them.

Since the cleavage fracture unit size corresponds closely to the lath packet width, it can be assumed that the high-angle boundary of the lath packet, rather than the low-angle boundary of a lath, is the first strong barrier to be traversed by a microcrack. As yield strength depends on carbide spacing (Figure 3), and no dependence on grain size or lath packet width could be obtained, it is obvious that the fracture strength cannot be calculated according to Petch equation nor can the calculations presented by Cottrell [13] be followed. However, an estimate for fracture stress can be obtained by using the Griffith equation [14].

$$\sigma_{fG} = \left[\frac{4E\gamma_p}{\pi(1-\nu^2)d}\right]^{1/2} \tag{5}$$

Using a value of 1.5 Jm^{-2} for γ_p [9] and 1.33 µm for d, a value σ_{fG} = 573 MPa is obtained. This value corresponds to the situation where $\lambda^{-1} = 0$, i.e. no carbides are present. The calculated value of fracture strength is well above the corresponding room temperature yield strength value of 275 MPa (See Figure 3).

If d in equation (5) is substituted with the smallest area which is surrounded by MC-carbides, i.e. with the MC-carbides spacing L_A, a considerable increase in calculated fracture strength as well as in the difference $\sigma_{fG} - \sigma_y$ is obtained with decreasing carbide spacing, as shown in Figure 5. This indicates decreasing values of DBTT, which is, however, contrary to the observations. If DBTT values are plotted as a function of yield strength a linear relationship showing increasing DBTT with increasing yield strength is obtained. This behaviour suggests a decreasing difference between fracture strength and yield strength with decreasing carbide spacing. To a first approximation it can be assumed that $\sigma_f = \sigma_y$ at any temperature when the deformation mechanism changes from Orowan looping to dislocation cutting of carbides (see Figure 4), although this assumption is not exactly true. Then σ_f can be drawn as straight line as a function of λ^{-1} from σ_f = 573 MPa at $\lambda^{-1} = 0$ to σ_f = 1010 MPa at λ^{-1} = 76 μm^{-1}, if the further assumption of a linear relationship is made. The difference $\sigma_f - \sigma_y$ expresses the amount of strain hardening and plastic work which is required for fracture nucleation and initial growth. On the other hand, the value of $\sigma_f - \sigma_y$ can also be considered to express how much we have to decrease (or increase) temperature from room temperature in order to achieve DBTT. This is the reason for the observed increase in DBTT-values with decreasing carbide spacing, i.e. toughness is reduced although the fracture strength is increased with finer carbide dispersion.

The above explanation holds for Charpy V DBTT-values, as this test measures mainly the nucleation and initial growth of microcracks. Another explanation for the dependence of NDTT on carbide spacing, however, must be sought because the Pellini drop-weight test measures crack propagation. Although linear, the observed relationship between NDTT and λ^{-1} differs somewhat from that of DBTT and λ^{-1}, as is seen in Figure 4. The difference between DBTT and NDTT is larger with larger carbide spacing and reduces to zero when the smallest values of spacing are approached.

When the carbide spacing is large, excessive plastic deformation at around room temperature can occur. Once a microcrack has been initiated it is effectively blunted and arrested due to mobile dislocations. Thus the temperature must be decreased to a rather low value before the plastic deformation becomes so difficult that crack blunting does not occur when a microcrack penetrates through the lath packet boundary, and that there is also enough elastic energy for further crack propagation. This unstable propagation, once started, proceeds at lower stresses and higher temperatures than the initiation requires [15]. When the carbide spacing is small, the dislocations are tightly locked and hence larger stresses and/or higher temperatures are needed for producing plastic deformation. Thus cleavage crack initiation can occur at higher temperatures, and as the

relative strength of grain boundaries is now smaller, there is not much difference between crack initiation and propagation and hence between DBTT and NDTT. This problem is more thoroughly discussed in reference [15].

CONCLUSIONS

The present results indicate that even in such a complex alloy as quenched and tempered secondary hardening Cr-Mo-V steel, the changes in the planar interparticle spacing of fine MC-carbides alone determines the changes in yield and fracture behaviour during tempering. In addition to the carbide spacing the lath packet size, which is rather independent of heat treatments, contributes to the fracture stress required for nucleation and initial growth of cleavage cracks. The latest theoretical modifications of the Orowan equation are well applicable in predicting the yield strength, but the Hall-Petch type equations are not valid, as no dependence on grain sizes was observed.

ACKNOWLEDGMENTS

We are grateful to Dr. Jarl Forstén for his continuous interest and valuable discussions in every stage of this research. This work was done under the auspices of the Ministry of Trade and Industry. The financial support of the Eemil Aaltonen Foundation and Suomen Kulttuurirahasto (K.T.) is also gratefully acknowledged.

REFERENCES

1. IRVINE, K. J., J. Iron and Steel Inst., 200, 1962, 820.
2. PETCH, N. J., J. Iron and Steel Inst., 174, 1953, 25.
3. ARMSTRONG, R. W., Phil. Mag., 9, 1964, 1063.
4. FOREMAN, A. J. E., HIRSCH, P. B. and HUMPHREYS, F. J., in "Fundamental Aspects of Dislocation Theory", 2, N.B.S. Publ. No. 317, Washington D.C. 1970, 1083.
5. KELLY, P. M., Int. Met. Rev., 18, 1973, 31.
6. BACON, D. J., KOCKS, U. F. and SCATTERGOOD, R. D., Phil. Mag., 28, 1973, 1241.
7. HAHN, G. T. and ROSENFIELD, A. R., Acta Met., 14, 1966, 1815; Trans. Met. Soc. AIME, 239, 1967, 668.
8. GLADMAN, T., HOLMES, B. and McIVOR, I.D., in "Effect of Second-Phase Particles on the Mechanical Properties of Steel" Iron and Steel Inst., London, 1971, 68.
9. HORNBOGEN, E. and STANIEK, G., J. Mat. Sci., 9, 1974, 879.
10. McCOMBS, J. B., GOLLAND, D. I. and MAYER, G., Mat. Sci. Eng., 15, 1974, 275.
11. TÖRRÖNEN, K., To be published.
12. ASHBY, M. F., in "Physics of Strength and Plasticity", MIT Press, Cambridge, Mass., 1969, 113.
13. COTTRELL, A. H., Trans. Met. Soc. AIME, 212, 1958, 192.
14. GRIFFITH, A. A., Phil. Trans. Roy. Soc., A221, 1920, 163.
15. KOTILAINEN, H. and TÖRRÖNEN, K., ICF 4, Waterloo, 1977.

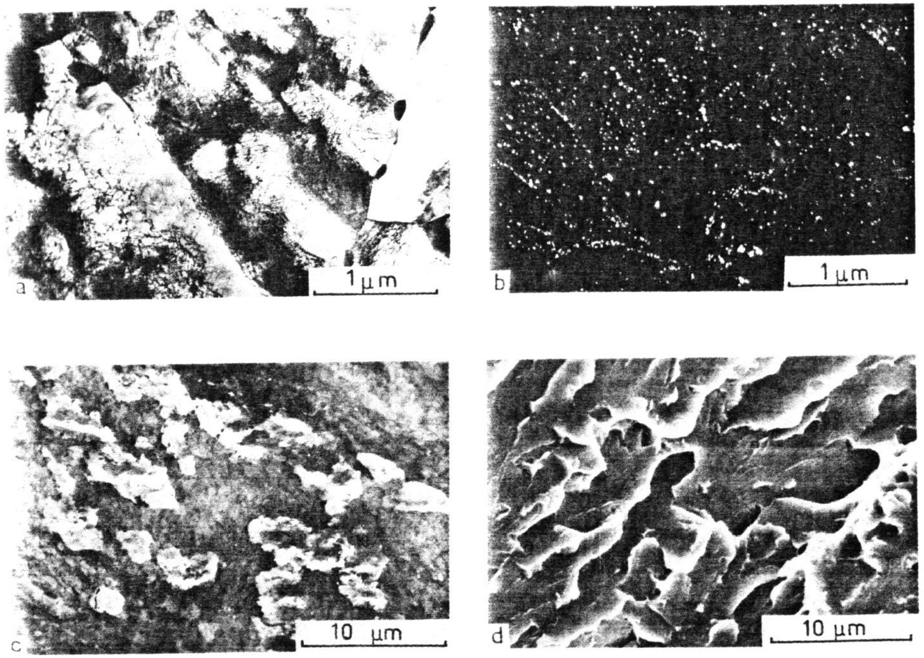

Figure 1 Typical Features in Microstructure and Fracture Surface Corresponding to a Hollomon-Jaffe Tempering Parameter Value of 20500

(a) Bright-Field Electron Micrograph
(b) Dark-Field Electron Micrograph Showing MC-Carbide Distribution
(c) Dark-Field Electron Micrograph Showing the Lath Packet Size
(d) Scanning Electron Micrograph Showing Cleavage Fracture Surface

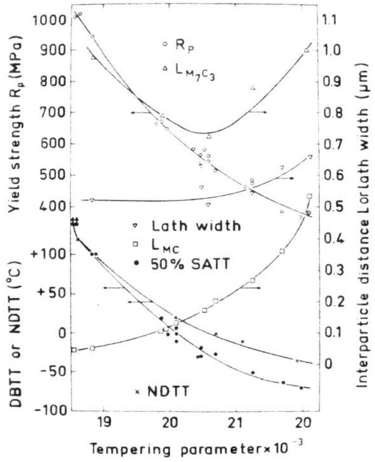

Figure 2 The Effect of Tempering on Microstructural Features and Mechanical Properties Given as a Function of the Hollomon-Jaffe Tempering Parameter

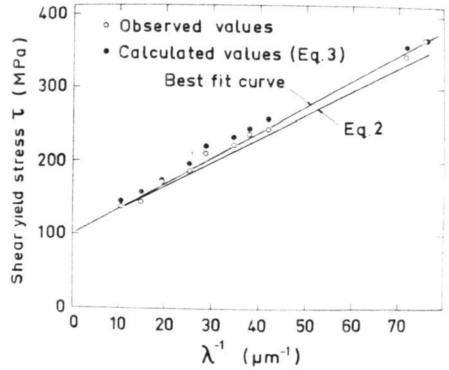

Figure 3 The Shear Yield Stress as a Function of Planar Spacing of MC-Carbides

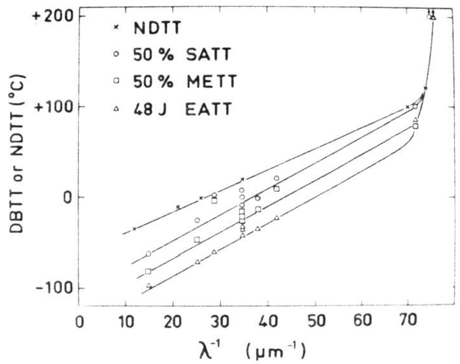

Figure 4 The Charpy V DBTT and Pellini NDTT as a Function of Planar Spacing of MC-Carbides

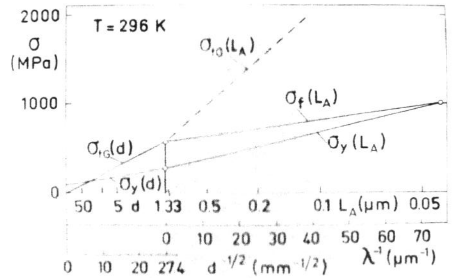

Figure 5 The Yield and Fracture Stress as a Function of Grain Size d and Carbide Spacing λ